Eur. Phys. J. D **20**, 557–563 (2002)
DOI: 10.1140/epjd/e2002-00154-7

THE EUROPEAN PHYSICAL JOURNAL D

Charge transport in a polypeptide chain

S.-Y. Sheu[1,a], D.-Y. Yang[2], H.L. Selzle[3], and E.W. Schlag[3,b]

[1] Department of Life Science, National Yang-Ming University, Taipei, Taiwan
[2] Institute of Atomic and Molecular Science, Academia Sinica, Taipei, Taiwan
[3] Institut für Physikalische und Theoretische Chemie, TU-Muenchen, Lichtenbergstrasse 4, 85747 Garching, Germany

Received 1st February 2002 / Received in final form 26 May 2002
Published online 13 September 2002 –

Abstract. Charge transport is one important example of signal transduction in a protein which is responsible for action at a distance, and is a fundamental process in biochemical action. A model is presented in which electronic effects interact with motional processes to combine into a bifunctional model. This model is investigated with new detailed molecular dynamics calculations and successfully explains such action at a distance.

PACS. 82.39.Jn Charge (electron, proton) transfer in biological systems – 83.10.Mj Molecular dynamics, Brownian dynamics

1 Introduction

Recently, charge conductivity of a protein molecule has become of general interest due to the fact that these systems could be classified as molecular wires. It is also of interest for the engineering of molecular devices, and the transduction of charge by molecules, which leads to molecular logic gates etc.

Schlag and his coworkers [1] have recently undertaken direct femtosecond measurements to investigate charge transfer processes along pure polypeptides, without attaching donors or acceptors. They employed only natural amino acids where one of these amino acids contains a natural chromophore, *i.e.* trypotophan. Charge is introduced into the system *via* photoexcitation. In their experiment, they found that charge transport through these model polypeptides could be extremely efficient for some choices of amino acids, or partially blocked in special cases of "blocking" amino acids. This process is modeled by a hopping mechanism between neighboring amino acids whose energies are pure electronic local energies. These energies are estimated in zero order from the ionization energy of the individual amino acids. The hopping then proceeds to a final low accessible electronic energy site, which may not have the lowest energy in the chain. This model has been successfully tested against some 20 polypeptides.

The polypeptides charge transfer experiments present some conceptual problems such as that the electronic energy landscape between amino acids, which typically leads to jumps of some 0.2–0.5 eV between two nearby amino acids. Here the jump process corresponds to some 2–5 fs for charge to transport. In reference [1], a direct timing measurements for a whole series of model systems, however, lead to a waiting time for a single jump in the 200–300 fs range, for a coupling energy of some 70 meV. Hence a model exhibiting two apparently discordant features are required. We need to have intermediate coupling permitting some residence of the charge on each amino acid, but at the same time we need to have strong coupling to pass the charge to the next amino acid. We proposed a new model where the details of mobility of a single charge in polypeptide chains was given by Baranov and Schlag [2] which involves two coupling regimes. The carbamide group of each amino acid is stiff, and very loosely hinged to the next amino acids. At this hinge carbon the two angles ϕ and ψ define the orientations of these two amino acids in respect to each other (Fig. 1). Over a very large range of angles this hinge motion is a nearly free rotation with virtually no potential energy restrictions except at their respective limits. This range is given in the Ramachandran plot [3].

Ab initio computations [2] show that even a pair of two identical amino acids will have an ionization energy asymmetry of some 0.6 eV due to the natural asymmetry of the C-side and the N-side of each amino acid (Fig. 1). For the ionic species in a small range of ϕ and ψ, when the carbonyl groups of the neighboring amino acids, around a C_α-hinge, are some 2.87 Å apart between O–O atoms, the electronic energy difference approaches a minimum. For the symmetric approach of the carbonyls, a neutral from one side and an ion from the other side an isoenergetic state exists in both units. These two states are strongly correlated and form one hybridized state. This is then the

[a] e-mail: sysheu@ym.edu.tw
[b] e-mail: schlag@ch.tum.de

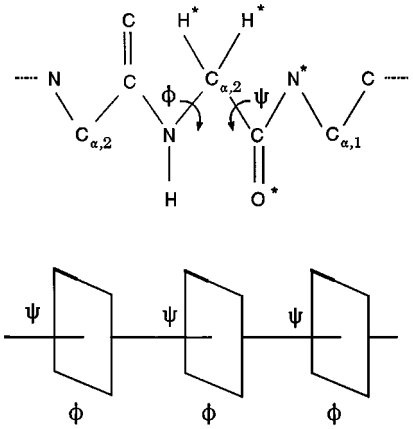

Fig. 1. Bifunctional model for charge transport along a polypeptide. The C_α atom joined between two nearby amino acids contains two torsion angles ϕ and ψ which constitute the Ramachandran plot. The motion inside the phase space follows a stochastic process. The injected electron dumped its energy to the ψ-axis which corresponds to a motion of virtual particle in the phase space till it reaches a proper ϕ and ψ angles and then waiting for jump to next nearby amino acid.

firing state for charge hopping. Hence this model suggests that we have strong coupling in a small range of ϕ and ψ in the Ramachandran plot leading to charge hopping [4]. The rest of the time the amino acid can freely rotate within a certain domain of the Ramachandran plot. Hence this has now formed the bifunctional model. Note that our model is based on a particle picture in contrast to a tunneling model [5].

Extending our bifunctional model to study the chemistry of action at a distance problem, such as charge transfer over long distance (molecular wires), is now an interesting problem. The local excitation at one end of a molecule and chemical reaction far away at the other end of a molecule is not treated in the conventional theory of reaction kinetics [6]. Traditional reaction rate theory is local, where chemical reaction proceeds on the site of excitation – we might refer to this as *proximal* kinetics. In contrast chemical reaction only at a distance may be referred to as *distal* kinetics. Some proteins are here seen to facilitate the charge transport process and act as a molecular wire. In this situation the protein can even be a logic gate triggered by the charge transport process and that triggered with very small energy such as found in a redox process.

Typical charge transport mechanism for charge transport along a polypeptide chain is based upon the nonadiabatic ET rate [7] between residues along the protein backbone. In contrast our bifunctional model contains two states, a "rest" and "fire" mechanism, and includes protein dynamic effects in addition to electronic effects to facilitate charge transfer in proteins. The motion of the rotors around a C_α-hinge is taken as a virtual particle moving inside a subregion called Baranov-Schlag (BS) box [8] in the Ramachandran plot. An entropy barrier dominates escaping from this BS box with a gate on its perimeter.

In the gas phase, a molecular dynamics (MD) simulation result shows that using our bifunctional model the charge migrates along the polypeptide chain very efficiently as also observed in mass spectroscopy [9]. The flow of charge in isolated polypeptides is characterized by an extremely efficient transport mechanism, nearly 100% proceeding to the final site, starting from the C-terminus. On the contrary and as a surprise, in the water system, the efficiency is found to be extremely small – we have two orders of magnitude in efficiency to be accounted for as a result of the change of medium. In this paper, we apply our bifunctional model to charge transport in the solvated polypeptide system. The successful escape should be counted before vibration modes and solvent modes set in. In other words, we only consider the carbonyl groups collision within the vibration energy dissipation time.

For the solvated MD computations, not all initial configurations leads to a firing state, but instead a fraction of initial states is dissipated, leading to an efficiency in the process of less than unity. Based on the superexchange model [10] , electron transfer rate is proportional to a distance dependent exponential form $Ae^{-\beta R}$ where the β-value is the distance decay factor and R is the charge transport distance between redox active sites. Here A is the pre-factor. Similarly such a distance dependence charge transfer rate is observed for charge transport in DNA and the β-value is between 0.1 and 1.40 Å^{-1} (Ref. [11]). For the α-helix such as myoglobin, its β-value is 1.3 Å^{-1}. A β-sheet, for example Azurin, shows a β-value of 1.0 Å^{-1}. The protein interestingly shows a very much higher charge transport efficiency as an isolated molecule in the gas phase, the loss in water we attribute here, on the basis of our model calculations, being due to a water barrel effect.

Based on Marcus rate theory [12] and various other possible ET pathways [13] for proteins, Beraton and Onuchic *et al.* [7] were able to obtain a β-value. We here consider the question of linking our efficiency obtained in the MD computations to the experimentally observed values of β in real proteins. Here we compute, based on our bifunctional model, the theoretically predicted β-value which we then compare to experimental data. We introduce a new local heating MD method which enables the study of these new possible effects and which is close to the physical model. The final result confirms our bifunctional model and dynamics contribution to charge transport in proteins and develops efficiencies and thus β-values which closely correspond to the experiment.

2 Bifunction model

We first consider an M amino acids polypeptide chain. Each amino acid contains a C_α-atom, *i.e.* a hinge between the amino acids and at each C_α-hinge there are two torsion angles, *i.e.* $\phi_{i-1,i}$ and $\psi_{i,i+1}$. Each pair of ($\phi_{i-1,i}$, $\psi_{i,i+1}$) constitutes a 2D-phase space, *i.e.* Ramachandran plot, as shown in Figure 1. Based on the experimental conditions in reference [14], the photoionized charge is initially injected into a carbamide group and its energy is transferred

to the two rotational degrees of freedom of the C_α-hinge and this charge is waiting in the $(\text{carbamide})_i$ residue until the $(\text{carbamide})_{i+1}$ group rotates to a certain angle and distance. Then the charge is transferred with zero barrier height and the electronic hopping rate is on the time scale of electronic correlation. Note that the charge is first excited to an electronic excited state and the excess energy is carried by the charge. When it moves to an adjacent carbamide group, the charge dumps part of its energy to the rotational degrees of freedom of the next carbamide group due to the energy conservation. The rotational period on the C_α-hinge is typically about 150 fs. This process is iterated until the charge reaches the N-terminal of the polypeptide chain, where then chemical reaction can occur.

Baranov and Schlag [2] have shown that for one particular angular configuration where the carbonyl groups of neighboring amino acids approach to a critical distance, there is an orbital degeneracy leading to a hybrid state for the charge species. This narrow range of angles then leads to facile charge transfer and thus presents a firing configuration. Hence the charge system can rotate over a phase space of large angular range as isolated species, but at a small subsection of this phase space firing sets in. This motion is mapped into the Ramachandran plot as a stochastic motion in phase space with torsion angles ϕ and ψ. There is a subregion, *i.e.* a gate, which corresponds to specific ratchet angles inside the Ramachandran plot. The waiting process is then becoming an escape process inside a 2D disk with a gate [8]. The asymmetry of the hopping rate will make the electron transport to the acceptor more effective. The entropy driven escape process is pictured as charge dumping its energy to the rotational degrees of freedom of the next site before vibration motions become active.

3 Escape process

In this section we consider the possible escape processes inside Ramachandran plot. The most probable regimes are the following three.

3.1 Quantum regime

In this section, we study the quantum escape rate of a virtual particle escaping out of a 2D disk. By applying the phase space theory in unimolecular reaction, the flux of the particle passing through the gate part [8] of the BS box inside the Ramachandran plot is decomposed into cells and each cell size satisfies the uncertainty principle. The reaction rate in canonical ensemble, based on the transition state theory, is then defined by phase space cell change. This transition rate in our case is equivalent to the particle escape rate.

In the phase space version of the Ramachandran plot, we can imagine that a particle moves ballistically inside a rectangular box. This ballistic motion occurs only if the two rotations contain energy of some 0.2–0.5 eV. In this regime, the escape rate constant becomes

$$k = \frac{1}{2\pi V_{\phi\psi}} \left[\Delta\psi\, \omega_\phi \sqrt{1 + \frac{I_\psi}{I_\phi}\left(\frac{\omega_\psi}{\omega_\phi}\right)^2} + \Delta\phi\, \omega_\psi \sqrt{1 + \frac{I_\phi}{I_\psi}\left(\frac{\omega_\phi}{\omega_\psi}\right)^2} \right] . \quad (1)$$

In equation (1), $V_{\phi\psi}$ is the phase space volume (see Fig. 1), $\Delta\phi$ and $\Delta\psi$ are gate lengths in ϕ and ψ dimensions, respectively. I_ϕ and I_ψ are the corresponding inertial moments. In a special square box, these two rotors have the same rotation frequency $\omega_\phi = \omega_\psi$, equivalent gate size in each dimension $\Delta\phi = \Delta\psi$, and the ratio of the length of the gate part relative to the perimeter length of the BS box is $\theta/2\pi = \Delta\phi/2\phi$ (here $\phi = \psi$), the transition rate expression is simplified into

$$k = \frac{2\sqrt{2}}{\pi} \frac{\omega_\phi}{\phi} \frac{\theta/2\pi}{1 - 4(\theta/2\pi)^2} . \quad (2)$$

The frequency part of the escape rate is in the range of 100 fs. Note that the activation part of the escape rate only depends on the relative gate-opening angle $\theta/2\pi$ and, hence, the escape process is entropy controlled. For a small gate size, *i.e.*, $\theta/2\pi \to 0$, the transition rate approaches

$$k \sim \frac{2\sqrt{2}}{\pi} \frac{\omega_\phi}{\phi} \frac{\theta}{2\pi} \quad (3)$$

and is proportional to the first order of the gate size.

Our MD simulation results [8] show that the torsion angle ranges are $\phi = 95^\circ$ and $\psi = 116^\circ$ and gate sizes are *ca.* $\Delta\psi = 43.925^\circ$ and $\Delta\phi = 25.1^\circ$. The corresponding escape time which is the inverse of the escape rate are $\langle t \rangle_{300\,\mathrm{K}} = 423$ fs.

3.2 Ballistic motion

We consider a billiard ball inside a 2D disk with a gate, which is a classical limit of the motion of the rotors in gas phase when the inertial moments are relative large or the polypeptide chain is long.

The mean free time for the billiard motion between two successive collisions within the disk wall with velocity v can be defined as $t_r = \langle R \rangle / v$. Here $\langle R \rangle$ is the mean free path for the billiard ball freely traveling inside the disk, with radius R, before colliding the disk wall and can be estimated as $\pi R/2$. We obtain the escape mean first passage time as $\langle t \rangle = t_r/(\theta/2\pi)$.

Note that, in the phase space theory, the velocity v of the billiard ball inside the 2D disk is equivalent to the oscillation frequency of the rotor ω. The total energy of the rotors , *i.e.* $I_\phi \omega_\phi^2/2 + I_\psi \omega_\psi^2/2$, is the input energy and is equivalent to $k_\mathrm{B}T$. So that each degree of freedom owns energy $k_\mathrm{B}T/2 = I_\phi \omega_\phi^2/2$. Note that these two rotors

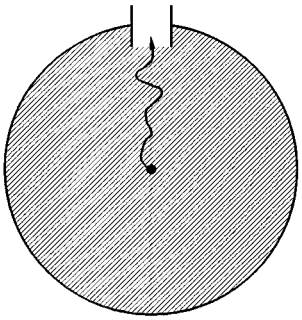

Fig. 2. 2D disk for a diffusion motion. Assuming that the Brownian particle moves inside a 2D disk with a static gate on its perimeter.

are assumed equivalent. Hence the mean free time can be expressed in terms of temperature (or input energy) as $t_r = (\pi/2)\sqrt{I_\phi/k_\mathrm{B}T}R$. It turns out that the final result of the escape time then becomes $\langle t\rangle = (\pi/2)(\phi/\omega_\phi)/(\theta/2\pi)$.

3.3 Diffusion motion

Solvent dynamic effects may slow down the virtual particle motion inside the BS box. This exhibits a diffusion regime for rotary motion inside BS box. As an alternative approach we consider diffusional motion of the particle inside a 2D disk (see Fig. 2) and the particle is initially thermal distributed inside the disk. The equation of motion of the particle satisfies a 2D Smoluchowsky equation

$$\frac{\partial}{\partial t}\rho = D_0\nabla^2\rho + \int \mathrm{d}\Omega\sigma(\Omega,t)\rho(r,t),$$

where ρ is the particle density and σ term is the surface reaction kernel. This equation can be solved by a self-consistent method [8,15]. By using the undulated radiation boundary condition

$$\bar{H}(\theta(t)-\theta)k_0\rho(r,t) = 2\pi D_0 R\mathbf{r}\cdot\boldsymbol{\nabla}\rho(r,t)$$

where $\theta(t)$ can be any time-dependent gating function representing the gate part. In our bifunctional model, $\theta(t)$ is a time-independent function. k_0 is the particle reaction rate on the gate part and is chosen as infinite in a later stage of calculation, and D_0 is the particle diffusion constant. The other quantity $\hat{\mathbf{r}}$ is the unit vector from the center of the disk to its perimeter. The general solution can be obtained by following our self-consistent method and the escape time is obtained as

$$\tau = \sqrt{2}\frac{2\pi}{\theta} \tag{4}$$

where θ is the maximum opening angle of the gate and is small. Here the relative gate-opening angle is the same as the one obtained in equation (3). Note that τ is characterized by the time scale R^2/D_0 and is twice of the phase space result. Along the radial axis, there exists a 1D entropy potential surface. The angular part does not contribute to the entropy potential surface. Thus the surface diffusion part is replaced by a random walk along the θ-axis, which is like a random walk along a 1D segment with length 2π.

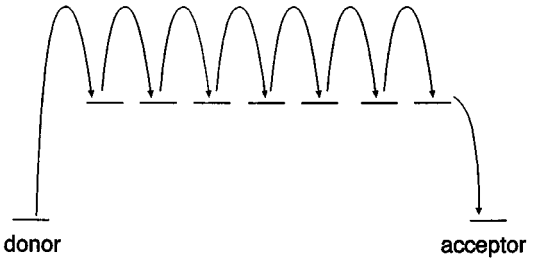

Fig. 3. Superexchange model. The typical superexchange model contains a donor and acceptor with bridge in between.

4 Efficiency and β-value

In this section, we investigate the charge transport efficiency based on our bifunctional model. The typical picture for charge transfer is that the rate goes as $A\,\mathrm{e}^{-\beta R}$. This is naturally justified for a superexchange [10] in which the level structure is shown in Figure 3 where the system has tunneled through a barrier with distance R.

First let us consider the peptide as a system of links or pearls (individual amino acids) on a string in which at the juncture we induce transfer to the next link. At the link juncture we assume a rate constant for charge transfer k_t and a rate constant for loss to the bath k_b. The fraction that continues as charge is thus $k_t/(k_t+k_b)$ after n links in the peptide, the fraction of charge that survives is $|k_t/(k_t+k_b)|^n$. The typical inter-residue distance in angiotensin is 3.7 ± 0.1 Å per unit. The total length of the chain is $R = 3.7n$. Here $a^n = \mathrm{e}^{n\ln a}$ where $a = k_t/(k_t+k_b)$ is the efficiency in equation (6). Thus, by writing in exponential form $\mathrm{e}^{n\ln a}$, one has

$$\beta = -\frac{\ln a}{3.7} \tag{5}$$

where the unit of β is Å^{-1}.

Assuming that $\beta = 1.25$ Å^{-1} or $k_b/k_t = 100$, then only 1% of charge transfer occurs at each step. The rest is lost to the phonon or heat bath. Similarly for $\beta = 0.19$ Å^{-1}, the ratio of k_b/k_t is 1.0. Both processes are equally fast. Note that over the small range of β from 0.2 to 1.3 Å^{-1} the ratio of rates goes from 50:50 to a transfer rate of only 1% of the total.

5 Molecular dynamic simulation: local heating

In this section, we demonstrate the motion inside the BS box with extensive MD calculations and also simulate the first passage time (fpt) distribution.

We first define the $\mathbf{C}_\alpha\mathbf{C}$ and $\mathbf{CX}$ vectors from C_α-atom to C-atom and from C atom to X atom, respectively. The X atom is any atom bound to the C atom

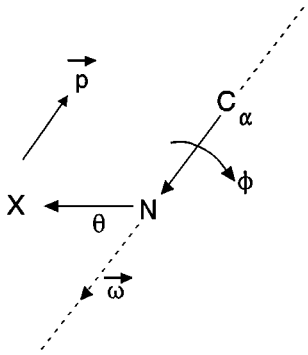

Fig. 4. Local heating model. The rotational axis of local heating along a C_α-hinge. X-atom is the local heated atom with torque $\boldsymbol{\omega} \cdot \mathbf{p}$ is the relevant moment of X-atom.

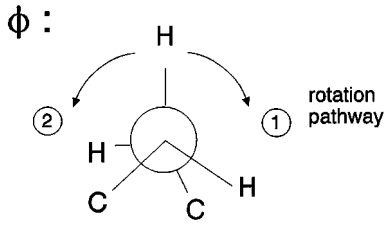

Fig. 5. Rotation pathway. There are two possible rotation pathways in our case.

(see Fig. 4). The vector orthogonal to the $\mathbf{C}_\alpha\mathbf{C}$ axis is $\mathbf{CX}_\perp$. In our MD simulation, we provide a charge energy ($E = I\omega^2/2$) which is *ca.* $E_{1667\,\mathrm{K}}$ to the atoms attached to the ψ axis, *i.e.* N, O, and H atoms with the excited angular velocity

$$\omega \times \left| \frac{\mathbf{CX}_\perp \times (\mathbf{CX}_\perp \times \mathbf{C}_\alpha\mathbf{C})}{|\mathbf{CX}_\perp| \cdot |\mathbf{C}_\alpha\mathbf{C}|} \right|^{-1}.$$

Here the unit of ω is changed into MD velocity and the charge energy or excitation energy E is in units of thermal energy. The rest of the atoms in the polypeptide chain are still kept at 300 K as the background temperature. Typically, in each simulation, 3 000 configurations have been chosen. Only part of the configurations have a successful O–O collision, *i.e.* O and O atoms come close to a certain distance, say 2.8 Å. We now define the efficiency as

$$\text{efficiency} = \frac{\text{successful configurations}}{\text{total configurations}}. \qquad (6)$$

In our simulation, the local heating method is implemented in a single site modified CHARMM 24 program [16]. Three different kinds of rotational direction (see Fig. 5) have been chosen such as positive (pathway 1), negative (pathway 2) and mixed (or random) pathway 1+2 rotation around the ϕ-angle. For random initial "trans" configuration of O–O atoms, the direction of rotation does not show any differences. However, for native initial configuration, the rotational direction or pathway directly affects the mean free path or mean free time [8]. The mean free time is reflected as the peak position of the fpt curve.

6 Results and discussion

In this section, we study the conclusive result of the bifunctional model for a polypeptide chain dissolved in water. We chose a polypeptide chain cut from the myoglobin helix with 20 residues and is called Mb_{20}. This polypeptide chain still keeps its α-helix structure. Then it is embedded in a water cluster. We first locally excite ψ-axis on a chosen site. In such a simulation, we run 3 000 configurations. Further comparison between the secondary structure supports our bifunctional model.

6.1 Distance dependent decaying factor: β-value

The local energy that we choose to heat up the ψ angle of the medial Mb_{20} dissolved in water is *ca.* 150 meV, *i.e.* $E_{1667\,\mathrm{K}}$. In our simulation a charge transports occurs from C-side to N-side. During the MD simulation, the first collision between O–O atoms within 2.8 Å is counted as a successful run. The water cluster contains 611 water molecules. After several picoseconds the equilibrium structure is reached. The MD calculations reflect a very low efficiency. Hence we have the interesting result that water, far from assisting charge transport here, seriously impedes the charge transport process in this model. This generates a β-value according to equation (5) of 1.3 Å^{-1} a value in good agreement with experiment. The thermal fluctuation and protein-solvent collision produce the noise part and will not be counted as efficiency. We fit our β-value by labeling the local efficiency with P_y^x, where x is the local heating site, at the residue site y. Since our local heating direction is, for example, from C-side of the C_α-hinge toward N-side of the polypeptide chain. We take the total efficiency such as $p_9^9 p_8^9 \times ... \times p_1^9 = A \exp\{-\beta \times 3.7 \times 9\} = 8.0 \times 10^{-11}$ in Table 1. On the other hand, we also have the total efficiency for the case with local heating site 8, *i.e.* $p_8^8 p_7^8 \times ... \times p_1^8 = A \exp\{-\beta \times 3.7 \times 8\} = 1.022 \times 10^{-8}$ in Table 2. The ratio for these two different local heating site situations gives a β-value equal to 1.31 Å^{-1}. The other extreme case, gas phase, in reference [17], shows a β-value equal to 1.158 Å^{-1} by using the same sequential transfer method adopted here.

6.2 Secondary structures

In this section we show that secondary structures have important additional effects on our transport model. Interestingly though the efficiencies are different for the native α-helix as compared to the β-sheet. The proximity of the groups in the α-helix are very close to the "firing" position, hence only very small motions are needed in the BS box to lead to charge transport. On the contrary the β-sheet is about three times more efficient than α-helix. In order to explain the higher efficiency of the β-sheet, we first show the fpt of the rigid β-sheet structure in Azurin. Then, we show that the solvated β-sheet has weaker H-bond than an isolated one. This breaks the strong interaction between chains inside β-sheet bound through H-bonds.

Table 1. Efficiency of Mb_{20} in water system (local heating site 9). Polypeptide sequence: Glu_1–Asp_2–Leu_3–Lys_4–Lys_5–Hsd_6–Gly_7–Val_8–Thr_9–Val_{10}–Leu_{11}–Thr_{12}–Ala_{13}–Leu_{14}–Gly_{15}–Ala_{16}–Ile_{17}–Leu_{18}–Lys_{19}–Lys_{20}. In this simulation there are 611 H_2O.

residue number	efficiency
1	0.05
2	0.06
3	0.03
4	0.11
5	0.055
6	0.20
7	0.015
8	0.67
9*	0.073
10	0.13
11	0.14
12	0.024
13	0.049
14	0.06
15	0.084
16	0.035
17	0.11
18	0.15
19	0.12

Table 2. Efficiency of Mb_{20} in water system (local heating site 8). Here the simulation condition is the same as Table 1. In stead, the local heating site is at residue Val_8.

Residue number	efficiency
1	0.042
2	0.042
3	0.025
4	0.127
5	0.079
6	0.21
7	0.25
8*	0.44
9	0.066
10	0.091
11	0.14
12	0.023
13	0.040
14	0.062
15	0.087
16	0.042
17	0.11
18	0.13
19	0.15

We choose a shorter model polypeptide chain from a synthesized β-sheet, which consists of a 12-mer, *i.e.* $V_5{}^DPGV_5$. In vacuum, this β-sheet contains four hydrogen bonds in Table 3. When it is dissolved in a 485 water cluster, the number of hydrogen bond pair is changed and the bond length is increased, *i.e.* weakened. We now pick up one pair of the hydrogen bond, for example V_4O–H–NV_{10}, and measure its relevant first passage time for the hydrogen bond to dissociate through its fpt curve at different temperatures.

Table 3. Hydrogen bond of $V_5{}^DPGV_5^*$ in gas phase. The hydrogen bond pair is expressed in terms of Aa — bB where a and b are the atom in residue A and B, respectively.

V_4–O	—	H–N–V_{10}
V_{12}–N–H	—	O–V_2
V_4–N–H	—	O–V_{10}
V_{12}–O	—	H–N–V_2

* The sequence of $V_5{}^DPGV_5$ is Ace–V_1–V_2–V_3–V_4–V_5–$^DP_6$–G_7–V_8–V_9–V_{10}–V_{11}–V_{12}–NH_2. (Ace = –$COCH_3$).

The dissolved β-sheet, hence, has much more flexibility than in vacuum. This is even seen here in the MD simulations. Therefore, the charge transport along each individual chain inside the β-sheet has the same efficiency as the α-helix has. But the total efficiency of the β-sheet is the geometric sum of each individual chain. Hence, for example in Azurin, the β-sheet contains about three chains. Its efficiency is about three times higher than each individual α-helix chain has. We hence have an efficiency of the β-sheet of *ca.* 0.0244, *i.e.* a β-value = 1.0 $Å^{-1}$. Therefore, for the theoretical predicted collision distance for firing, the calculated efficiency here predicts a β-value that corresponds closely to known experiments. This work suggests that, in contrast to some intuitive views, the charge transport in water is not necessarily optimal. Charge transport in an isolated environment such as in the gas phase can be some 100 fold more efficient. This theoretically calculated inefficiency agrees with experiment.

7 Conclusion

Protein or polypeptide chains show a new distal reaction scheme. Our bifunctional model shows that the experimental observation is an essential consequence of both local excitation and a special form of protein mobility. Our molecular single site dynamics simulation result makes it possible to pursue the motion of energy and charge down the chain and again confirms the bifunctional behavior of the charge transport process in solvated system.

The efficiency can even be transferred to charge migration in secondary structures and displays strong differences between the α-helix and the β-sheet. The β-sheet here is seen to be superior in charge transfer to the α-helix just as a result of parallel path and not intrinsically.

This work was supported by the Taiwan/Germany program at the NSC/Deutscher Akademischer Austauschdienst. SYS and DYY are supported by NSC Grants no. NSC-90-2113-M-010-001 and NSC-90-2113-M-001-048, respectively.

References

1. R. Weinkauf, P. Schanen, D. Yang, S. Soukara, E.W. Schlag, J. Phys. Chem. **99**, 11255 (1995); L. Lehr, T. Horneff, R. Weinkauf, E.W. Schlag, *Fs Dynamics after Local Photoionization: 2-phenylethyl–N,N-dimethylamine as*

a Model System for Non-Resonant Downhill Charge Transfer in Peptides (unpublished)
2. L.Ya. Baranov, E.W. Schlag, Z. Naturforsch. **54a**, 387 (1999)
3. G.N. Ramachandran, V. Sasisekharan, Adv. Protein Chem. **23**, 283 (1968)
4. E.W. Schlag, S.Y. Sheu, D.Y. Yang, H.L. Selzle, S.H. Lin, Proc. Natl. Acad. Sci. USA **97**, 1068 (2000)
5. *Electron Transfer – From Isolated Molecules to Biomolecules*, Advances in Chemical Physics, edited by J. Jortner, M. Bixon (John Wiley and Sons, New York, 1999), Parts 1 and 2, Vols. 106 and 107
6. T. Baer, W.L. Hase, *Unimolecular Reaction Dynamics: Theory and Experiments* (Oxford University Press, Oxford, 1996)
7. J.N. Onuchic, D.N. Beratan, J. Chem. Phys. **92**, 722 (1990); J.N. Onuchic, P.C.P. de Andrade, D.N. Beratan, J. Chem. Phys. **95**, 1131 (1991)
8. E.W. Schlag, S.Y. Sheu, D.Y. Yang, H.L. Selzle, S.H. Lin, J. Phys. Chem. B **104**, 7790 (2000)
9. R.A Zubarev, N.A. Kruger, E.K. Fridriksson, M.A. Lewis, D.M. Horn, B.K. Carpenter, F.W. McLafferty, J. Am. Chem. Soc. **121**, 2857 (1999); R.A. Zubarev, M.L. Nielsen, B.A. Budnik, Eur. J. Mass Spectrom. **6**, 235 (2000)
10. H.M. McConnel, J. Chem. Phys. **35**, 508 (1961); J.R. Miller, J.V. Beitz, J. Chem. Phys. **74**, 6746 (1981); A. Nitzan, J. Jortner, J. Wilkie, A.J. Burin, M.A. Ratner, J. Phys. Chem. B **104**, 5661 (2000); Y.A. Berlin, A.L. Burin, M.A. Ratner, J. Phys. Chem. A **104**, 443 (2000); M. Ratner, Nature **397**, 480 (1999)
11. S.L. Mayo, W.R. Ellis Jr, R.J. Crutchley, H.B. Gray, Science **233**, 948 (1986); J.R. Winkler, H.B. Gray, JBIC **2**, 399 (1997)
12. R.A. Marcus, J. Chem. Phys. **24**, 966 (1956)
13. B.S. Brunschwig, N. Sutin, J. Am. Chem. Soc. **111**, 7454 (1989); B.S. Brunschwig, N. Sutin, Comm. Inorg. Chem. **6**, 209 (1987)
14. P. Schanen, Ph.D. thesis, Technische Universität München, 1997
15. S.Y. Sheu, D.Y. Yang, J. Chem. Phys. **112**, 408 (2000)
16. B.R. Brooks, R.E. Bruccoleri, B.D. Olafson, D.J. States, S. Swaminathan, M. Karplus, J. Comp. Chem. **4**, 187 (1983)
17. S.Y. Sheu, E.W. Schlag, D.Y. Yang, H.L. Selzle, J. Phys. Chem. A **105**, 6353 (2001)